Journal of Radioanalytical and Nuclear Chemistry (2024) 333:705–715
https://doi.org/10.1007/s10967-023-09323-3

Biogenic harmony of biocompatible silver nanoplatforms using chamomile extract and apigenin-7-glucoside for solid tumor therapy

Adli A. Selim[1] · Islam M. Abdelmonem[2] · Mohamed A. Amin[3] · Basma M. Essa[4]

Received: 9 September 2023 / Accepted: 15 December 2023 / Published online: 29 January 2024

Abstract

This study focuses on tumor therapy using two biocompatible silver nanoplatforms of chamomile extract and its active ingredient apigenin-7-glucoside. Chamomile silver nanoparticles (Ch-AgNPs) and apigenin 7- glucoside silver nanoparticles (Ap-AgNPs) were synthesized and characterized using different analytical techniques. On a stable nanoplatform with spherical nanoparticles in a narrow size range, both Ch-AgNP and Ap-AgNP exhibit potent cytotoxic effects against two different cell lines (HepG2 and MCF7). The synthesized NPs were radiolabeled with ^{131}I giving high radiochemical purity. Biodistribution studies in tumor-bearing Albino mice showed higher accumulation in tumor sites compared to normal muscle. In conclusion, after further preclinical studies, both chamomile silver nanoparticles (Ch-AgNPs) and apigenin-7-glucoside silver nanoparticles (Ap-AgNPs) can be used as potential drugs for tumor theranostics.

Keywords Biogenic nanosynthesis · Chamomile · Apigenin-7-glucoside · Theranostic agents · Radioiodination

Introduction

Cancer is one of the most dangerous threats to human health and is considered the second leading cause of death for all human beings. The early stages of cancerous lesions are the most important steps for successful treatment. Choosing the right treatment for cancer patients faces many challenges, such as age, side effects, and patient compliance. Therefore, it is urgent to find targeted and personalized treatments. The possible uses of nanomaterials to improve human life and its environment are numerous [1]. One of the methods used to synthesize nanoparticles is environmentally friendly green chemistry, represented by plants, which has the advantage of overcoming the shortcomings of chemical and physical methods without the need for toxic chemicals, energy, pressure and temperature [2, 3]. Bioavailability is the amount and rate at which a drug is absorbed. The rate of absorption should be fast or slow depending on the treatment condition, which can be achieved by changing the physicochemical properties of the drug and the properties of the dosage form. Nano-formulations have many advantages, especially in botanical medicines, including improved bioavailability, reduced toxicity, enhanced pharmacological activity, etc. [4, 5]. Thus, nano-phytopharmaceuticals hold great future potential in enhancing activity and overcoming problems associated with herbal medicines. Chamomile, also known as Chamomilla recutita or Matricaria recutita, has a long history of use as an herbal remedy. The plant contains various biologically active compounds, including coumarins and sesquiterpenes. Flavonoids have also been identified in chamomile, with apigenin being the most abundant and contributing to the observed pharmacological properties of the plant's flowers, known as "Chamomillae flos" [6–8]. Developmental studies have been conducted to investigate the total apigenin content throughout the life cycle of both diploid and tetraploid forms of chamomile. The interest in chamomile research continues due to its reported anti-inflammatory, anti-viral, and particularly anticarcinogenic

✉ Adli A. Selim
adli_a_selim@yahoo.com

[1] Labeled Compounds Department, Hot Laboratories Centre, Egyptian Atomic Energy Authority (EAEA), Cairo 13759, Egypt

[2] Nuclear Chemistry Department, Hot Laboratories Centre, Egyptian Atomic Energy Authority (EAEA), Cairo 13759, Egypt

[3] Pt CELL for Pharmaceutical Industries Co., 10Th of Ramadan City, Cairo 44629, Egypt

[4] Radioactive Isotopes and Generator Department, Hot Laboratories Centre, Egyptian Atomic Energy Authority (EAEA), Cairo 13759, Egypt

properties [9–11]. Apigenin has been extensively studied for its anti-inflammatory and anticarcinogenic properties. It has been shown to inhibit the growth of various cancer cell lines and to induce apoptosis (programmed cell death) in cancer cells, making it a promising compound for cancer prevention and treatment. Apigenin has also been reported to have neuroprotective effects, as well as to improve glucose metabolism and insulin sensitivity [8, 12]. Theranostics in nuclear medicine exploit the properties of certain isotopes, such as ^{131}I, for imaging and therapy [13]. This approach helps identify specific molecular targets in patients, monitor treatment effects, and monitor potential toxicity. ^{131}I is one of the most commonly used radioisotopes in nuclear medicine. ^{131}I decays to extremely stable xenon-131 with a half-life of 8.03 days. Negative beta particles and gamma photons are released during the decay process. The average and maximum energies of primary beta emissions are 191.5 keV and 606.3 keV, respectively, while primary photons (gamma emissions) have an energy of 364.5 keV [14], and are therefore used for targeted radionuclide therapy (TRT) [15].

Experimental

Dry chamomile flowers were purchased from Haraz, Egypt. All other reagents were purchased from Sigma (St. Louis, MO) and were of analytical reagent grade or HPLC grade where applicable. Apigenin 7-*O*-glucoside (> 95% pure), were obtained from Sigma. HR TEM (Ted Pella, Redding, CA, USA), DLS (BIC, USA and PCS), Zetasizer (Beckman Coulter, Miami, FL, USA) were used for characterization of nanoplatforms. ^{131}I was obtained from RPF, EAEA, Egypt. NaI (Tl) γ-counter (SPECTECH, ST450 SCA, USA) for radioactivity measuring.

Extraction of chamomile extract

Dry chamomile flowers were weighed and crushed to fine powder (mesh 50). The chamomile flower powder was extracted in heat reflux extractor under stirring for 18 h, (Pt CELL for pharmaceutical industries) by hydroalcoholic solvent (water: ethanol ratio 3:1). After that, the suspension was filtered. The filtered aqueous extract was concentrated and dried in vacuum oven (Pt CELL for pharmaceutical industries) at 50 °C, whereas organic extracts were dried at room temperature and stored at − 20 °C until use.

Determination the content of apigenin-7-glucoside in chamomile powder extract by HPLC

The Content of Apigenin-7-glucoside in chamomile flowers and chamomile powder extract was determined by Waters HPLC Acquity Arc with PDA Detector, Pt CELL for pharmaceutical industries.

a- Chromatographic conditions:

Column:—Waters XSELECT C18, 5µ, (250 * 4.6) mm.
Flow Rate: 1.5 ml/min.
Detection Wave Length: 335 nm.
Injection volume: 20 µL.
Mobile phase:

(A) 5 mM KH_2PO_4 pH 2.5 by H_3PO_4.
(B) Acetonitrile: Methanol (65: 35) %

Time	(A)	(B)
0	75	25
2	75	25
15	15	85
18	75	25
25	75	25

b- Standard preparation:

- Accurately weigh 5 mg of Apigenin-7-glucoside standard.
- Transfer it to 100 ml volumetric flask.
- Add 80 ml methanol and sonicate for 10 min.
- Cool to room temperature and add methanol to the volume.
- Filter using syringe filter 0.22µ and discarding the first 5 ml of the filtrate.

c- Sample preparation:

- Accurately weigh 1 g of Chamomile powder extract.
- Transfer into Suitable flask fitted with reflux condenser and stirrer.
- Add 80 ml methanol then heat and reflux the mixture with stirring for 1 h.
- Cool to room temperature and filter then collect the filtrate into 100 ml volumetric flask.
- Complete to volume with methanol then take 30 ml into round flask fitted with reflux condenser and stirrer.
- Add 5 ml of NaOH solution prepared by dissolving 0.4 g NaOH in 5 ml water.
- Heat and reflux the mixture for 25 min then cool to room temperature. Adjust pH with HCl of 5 to 6.2.
- Transfer the solution to 50 ml volumetric flask then complete to volume with methanol.

- Filter using syringe filter 0.22 μ and discarding the first 5 ml of the filtrate.

d- Sample testing.

Accurately inject the standard solution for three times when the chromatographic system is stabilized under the condition. The RSD should be not more than 2.0%. Inject equal volumes of sample solution to the chromatograph, record the chromatograms and measure the peak responses of Apigenin-7-glucoside.

e- Calculation.

Calculate the percentage of Apigenin-7-glucoside taken by the formula:

$$Assay = \frac{Average\ area\ of\ test}{Average\ area\ of\ standard} \times \frac{Conc.\ of\ standard}{Conc.\ of\ test} \times Potency\ of\ standard$$

Synthesis and characterization of Ch-AgNPs and Ap-AgNP

First; 0.7 ml of 1 mM silver nitrate was added dropwise to 3 ml of 2 mM sodium borohydride, then mixed for 10 min to form AgNPs. Second; 0.5 mL of chamomile extract (5 mg/mL) or 0.5 mL of apigenin 7-glucoside (1 mg/mL) was added to the AgNPs and mixed well, then left for a day to form Ch-AgNPs or Ap-AgNPs. Ch-AgNP and Ap-AgNP platforms were well characterized using HR-TEM to determine shape and core diameter, DLS to determine hydrodynamic diameter, and Zeta Sizer to determine the zeta potential of the formed nanoplatforms.

Antioxidant capacity determination, DPPH assay

The antioxidant capacity of chamomile extract, apigenin 7-glucoside, Ch-AgNP, and Ap-AgNP was tested using the DPPH assay. Free radical scavenging activity by 2,2-Diphenyl-1-trinitrophenylhydrazine hydrate (DPPH) assay [16] and comparison of chamomile extract, apigenin-7-glucoside, AgNPs, Ch-AgNPs, and Ap-AgNPs in terms of antioxidant potency: first add 100 μL of freshly prepared DPPH reagent (0.1% methanol), then add 100 μL of sample into the well plate, and incubate at room temperature for 30 min in the dark. Measure the density of the reaction color at 540 nm using a FluoStar Omega microplate reader, and the result is expressed by the following equation:

$$\%RSA = \frac{A0 - A1}{A0} \times 100$$

*RSA is the radical scavenging activity, A0 is the absorbance of the control and A1 is the absorbance of the test.

Cytotoxicity assay

Cell lines: HepG2 and MCF-7 cell lines were obtained from ATCC through its Biologics and Vaccines Holding Company (VACSERA) in Cairo, Egypt. *Chemical reagents:* reagents RPMI-1640 medium, MTT and DMSO (Sigma Co., St. Louis, USA), fetal bovine serum (GIBCO, UK). For comparison, doxorubicin was used as a standard cancer drug. *MTT Assay:* Using the various cell lines described above, the inhibitory effect of compounds on cell growth was determined by MTT assay. This colorimetric assay is based on the conversion of yellow tetrazolium bromide (MTT) to a purple formazan derivative by mitochondrial succinate dehydrogenase in living cells.

Radioiodination of Ch-AgNPs and Ap-AgNP

[^{131}I]I-Ch-AgNPs and [^{131}I]I-Ap-AgNPs platforms were prepared by optimized values of the substrate (Ch-AgNPs or Ap-AgNP), chloramine-T (CAT), pH and time. First; the substrate was placed in a dark, sealed reaction vessel, then CAT was dissolved in ethanol to a concentration of 8.8 mM and added, followed by Na13I. All factors were studied as the following amounts: CAT amount (25–125 μg) at different pH ranges (6–10) and substrate amount (0.25–1.25 mL) over 5–60 min. After the reaction was complete, the reaction was terminated with 5 μL of sodium thiosulfate (190 mM). The reaction was monitored by RTLC technique by using methanol 70% as a solvent system and radiochemical purity was determined in the same way, where free iodide migrated at Rf = 0.6 to 1.00, while the iodinated platform at Rf = 0.00 remained at the origin. Then purified from any free iodide before in-vivo studies.

Radiolabeling yield = Total activity

(Rf = 0 - 1) - activity of free 131I (Rf = 0.6 - 1)

Biodistribution study of [^{131}I]I- Ch-AgNPs and [^{131}I] I- Ap-AgNPs

Animal biodistribution studies have been approved by the Ethics Committee of the Egyptian Atomic Energy Authority (EAEA). In this study, tumor-bearing Swiss albino mice weighing approximately 25–30 g were divided into five

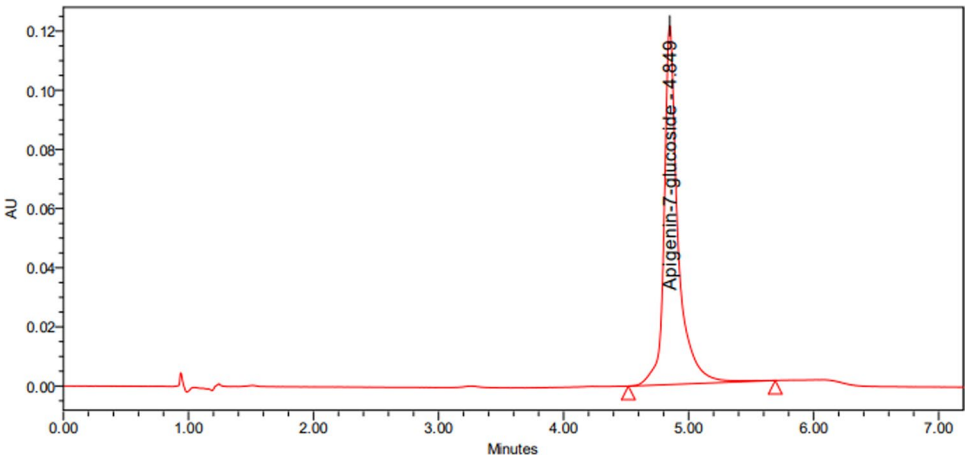

Fig. 1 HPLC of Apginin-7-glucoside

groups (5 mice per group). Each mouse was intravenously injected with [^{131}I]I-Ch-AgNPs or [^{131}I]I-Ap-AgNPs 10 µl at a concentration of 2 mCi, then the mice were anesthetized with isoflurane and weighed at different times (0.25, 0.5, 1.0, 2.0, 4.0 and 24 h)) after injection. Fresh blood, bone and muscle samples were collected in vials that were weighed first and counted, where the weight of bone, muscle and blood had to be 10, 40 and 7% of the total body weight, respectively [17–19], other organs and tissues were rinsed with saline and observed in the container, and counted with a NaI(TI) well-type γ counter to determine the radioactivity in each sample. All results were calculated using percent injected dose/gram organ (%ID/g organ).

Results and discussion

Extraction and purification of chamomile and Apigenin-7-glucoside

The retention time (Rt) for Apigenin-7-glucoside was quantitatively determined by injecting standard solutions of each into the UHPLC chromatographic column. The determined Rt for Apigenin-7-glucoside standards was 4.849 min (Figs. 1, 2, 3 and 4). The *Chamomile* extract was also subjected to HPLC separation (Fig. 3), which showed the presence of Apigenin-7-glucoside at the previously assigned Rt. Finally, the precipitated Apigenin-7-glucoside was identified similarly, the chromatogram showed 10.29% recovery of the total Apigenin-7-glucoside content in the original extract.

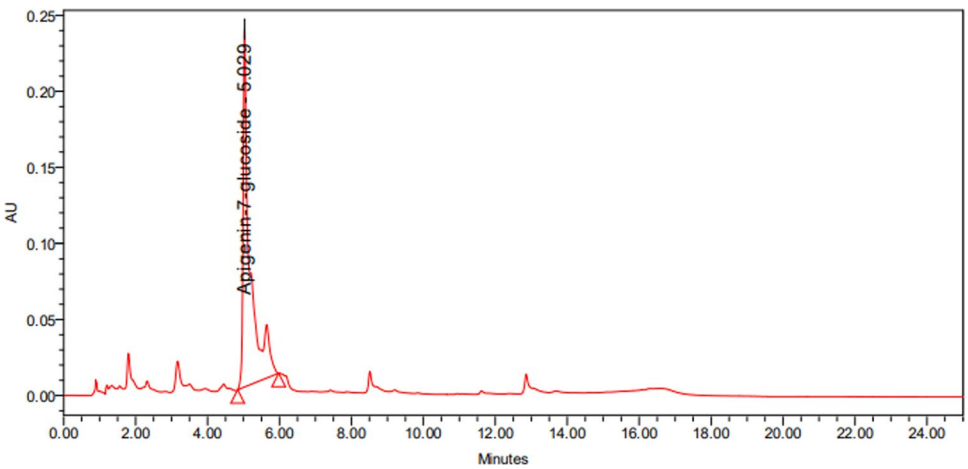

Fig. 2 HPLC of chamomile herb

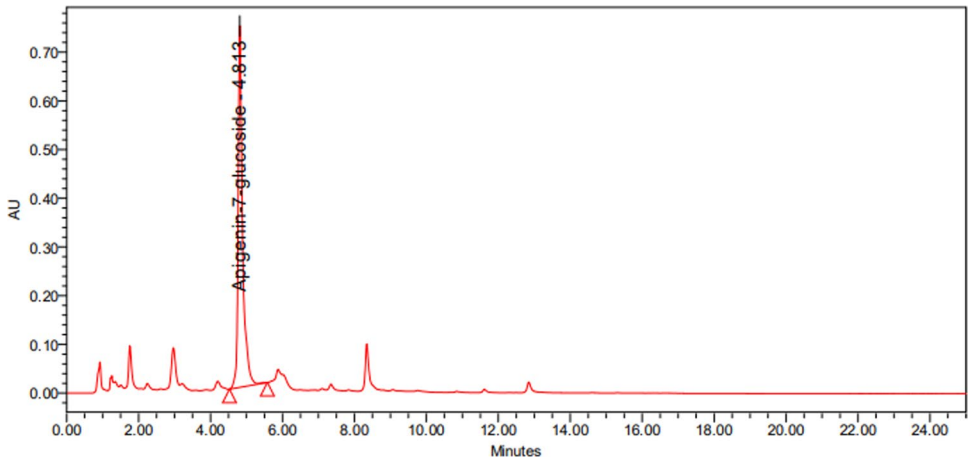

Fig. 3 HPLC of chamomile extract

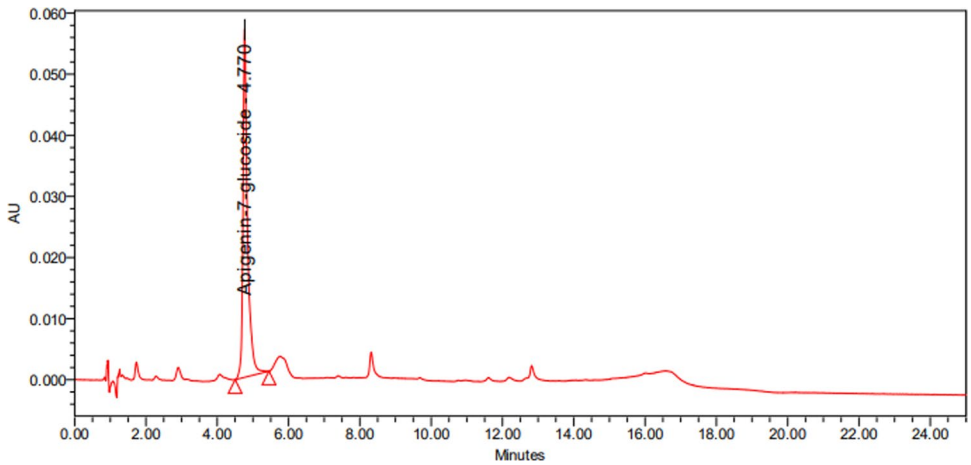

Fig. 4 HPLC of chamomile herb after extract

Synthesis and characterization of Ch-AgNPs and Ap-AgNP

Chamomile extract and apigenin 7-glucoside are well known antioxidants. AgNPs were formed from Ag ions using sodium borohydride as a reducing agent. Subsequently, chamomile extract and apigenin 7-glucoside were used to functionalize and stabilize the formed Ch-AgNP and Ap-AgNP, respectively. Figure 5, 6 show the average size of Ch-AgNPs and Ap-AgNPs determined using different techniques (TEM and DLS), respectively. TEM revealed spherical nanoparticles with mean diameters of 10 and 8 nm for Ch-AgNPs and Ap-AgNPs, respectively; while DLS showed mean hydrodynamic diameters of Ch-AgNPs and Ap-AgNPs were 357 and 308 nm, respectively, and their stability was determined by zeta potential which give values of 19.44 and 11.17 mV for Ch-AgNPs and Ap-AgNPs, respectively, indicating the stability of the colloidal nanoplatform. This stability may be due to the electrostatic repulsion created by the presence of charged surfaces.

Antioxidant capacity

One of the main causes of DNA damage is free radicals that represent the first stage of carcinoma, natural products consist of many of antioxidant source act as exogenous which stimulate function of the endogenous antioxidant system to prevent free radicals formation inside the body as its main responsibility [20, 21]. Chamomile was reported to induce apoptosis in cancer cells [22]. Ch-AgNPs showed the highest scavenging activity with IC_{50} of 5.88 ± 0.77 µL/mL followed by Ap-AgNPs with IC_{50} of 11.34 ± 0.61 µL/mL, while the value of IC_{50} for both apigenin 7-glucoside and chamomile extract > 1000.

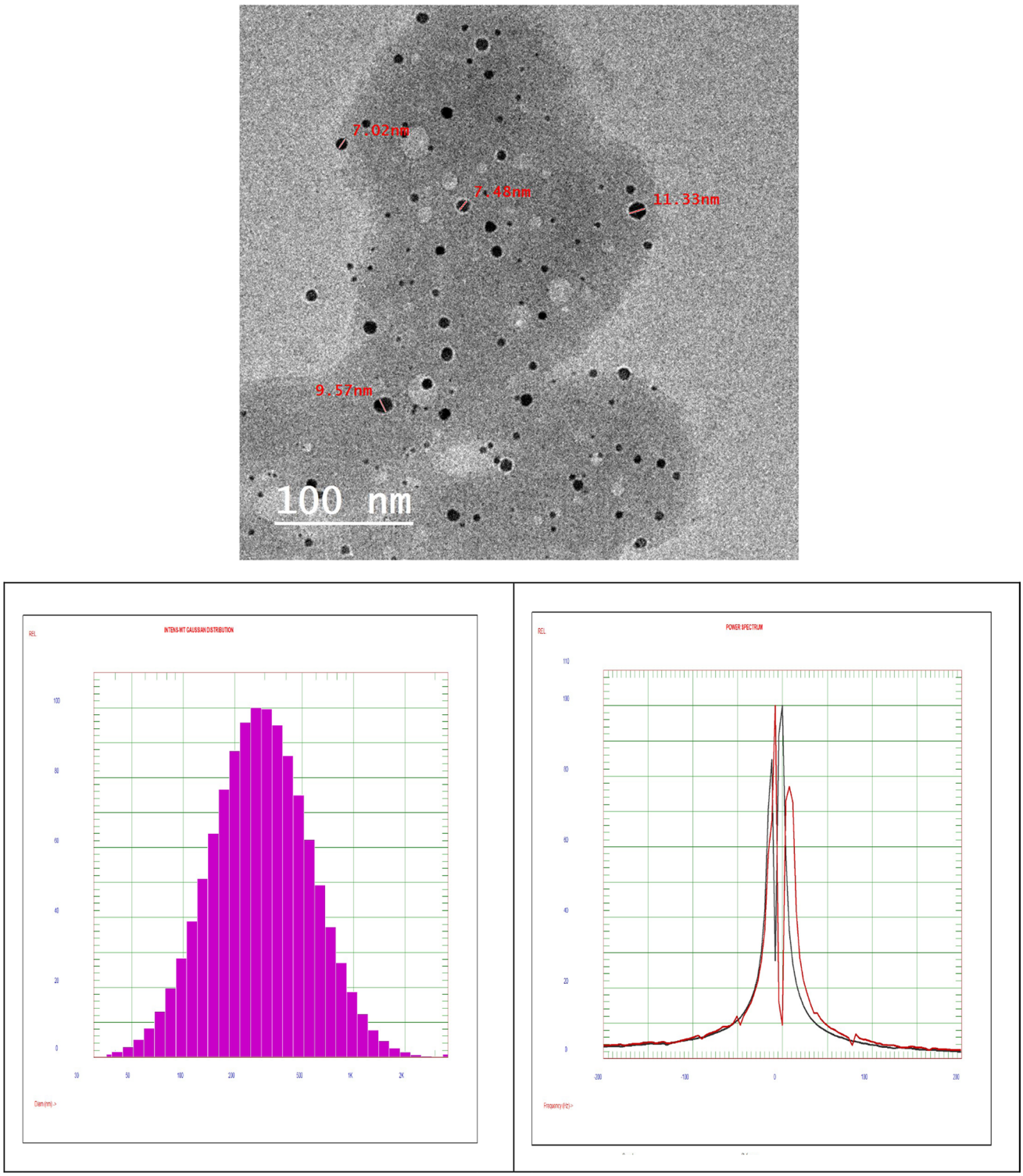

Fig. 5 Ch-AgNPs core diameter, hydrodynamic diameter and zeta potential

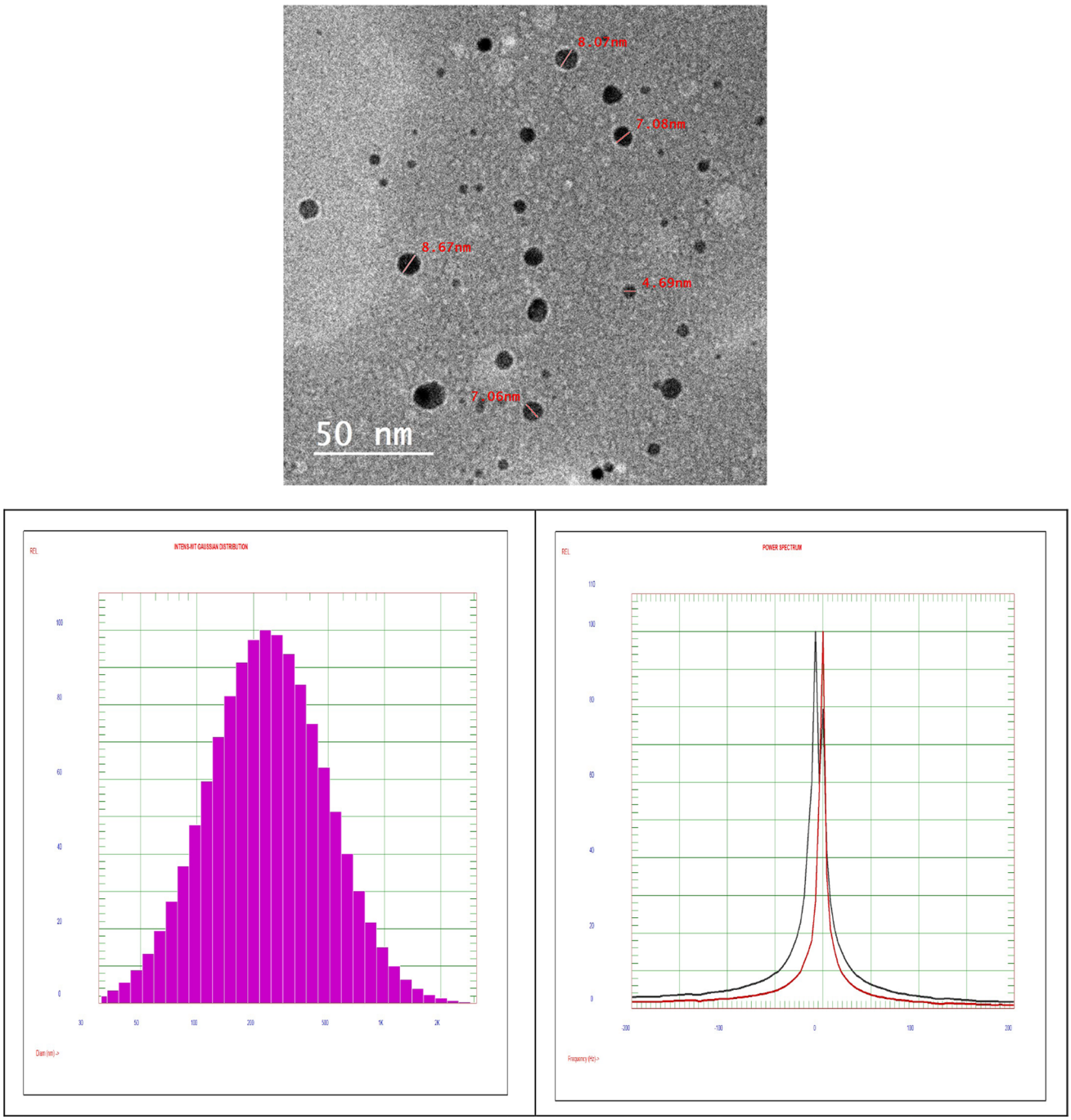

Fig. 6 Ap-AgNPs core diameter, hydrodynamic diameter and zeta potential

Cytotoxicity of the newly synthesized nano-platform against HepG2 and MCF-7

Liver cancer and breast cancer are the two most common types of cancer in humans. Therefore, we chose HepG2 and MCF-7 human cancer cell line models for testing. The cytotoxic activity of the synthesized NPs was tested against HepG2 and MCF-7 and compared with DOX (doxorubicin) as a known reference. The results showed that both nano-platforms (Ch-AgNPs and Ap-AgNPs) had high cytotoxic effects on both cell lines tested. The IC50 values of Ch-AgNPs against HepG2 and MCF-7 were 6.2 and 6.9 µg/mL, while the IC50 values of Ap-AgNPs against HepG2 and MCF-7 were 5.2 and 6.1 µg/mL, respectively.

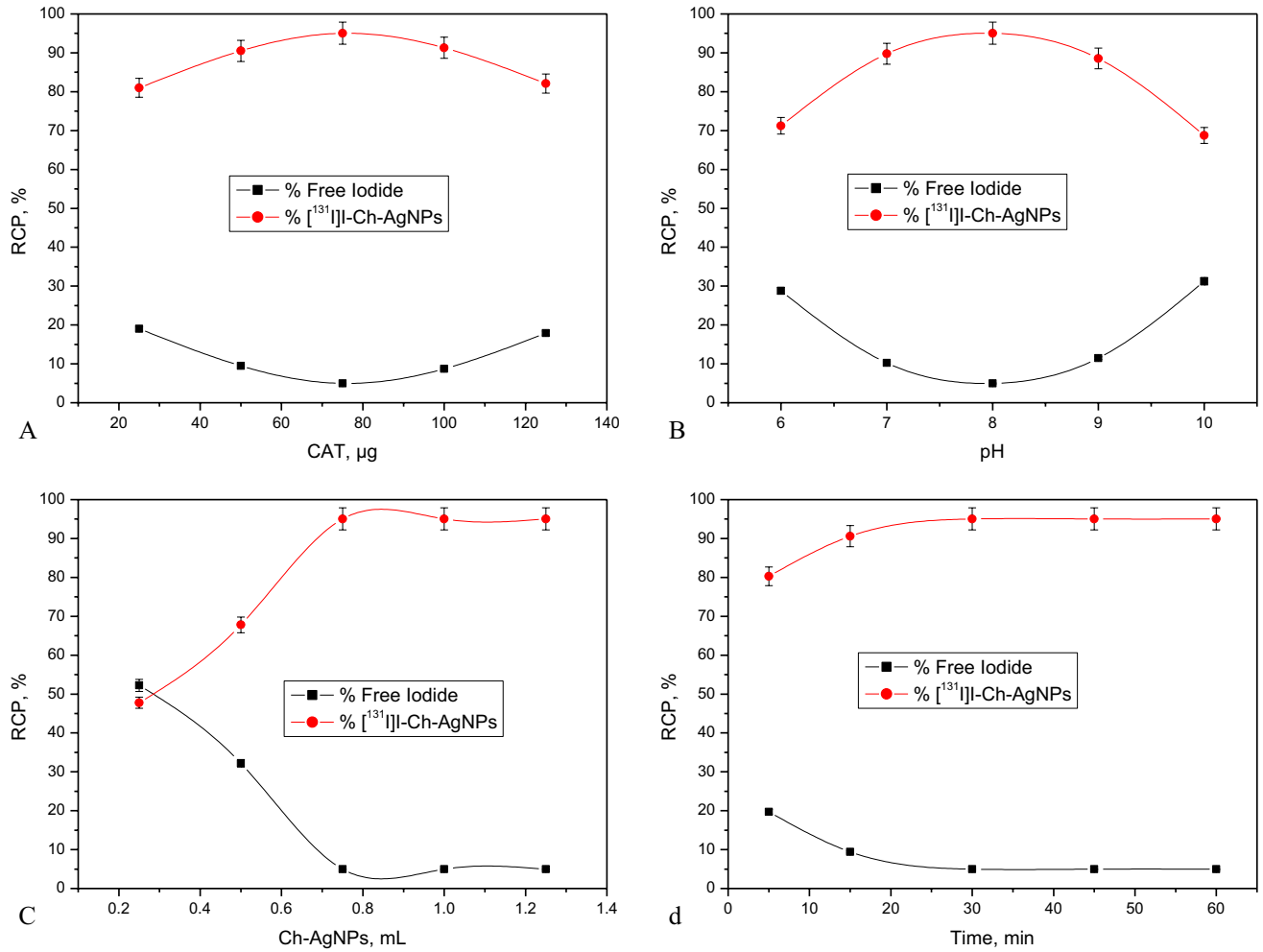

Fig. 7 Effect of reaction parameters on RCP of [^{131}I]I-Ch-AgNPs: a- CAT amount. b- pH, c- Substrate amount, d- Reaction time

Formation of [^{131}I]I-Ch-AgNPs and [^{131}I]I-Ap-AgNPs

The maximum RCP of 95.04 ± 2.85 and 97.36 ± 2.92% were obtained for both Ch-AgNPs and Ap-AgNPs, respectively. Briefly ([^{131}I]I-Ch-AgNPs), 1 mL total reaction volume by the addition of 5 µL Na^{131}I containing 2 mCi to a mixture of 750 µL of nano-platform and 75 µg CAT (2 CAT: 1 EtOH) at pH 8 at room temperature for 0.5 h; while in case of [^{131}I]I-Ap-AgNPs the same conditions were used with only 50 µg CAT. RCP was determined by means of TLC for each experiment. NPs were radiolabeled with ^{131}I by direct electrophilic substitution with CAT as the oxidant. The above-mentioned factors studied in this experiment are all affected by the reaction pathway. The highest RCP obtained depends mainly on the amount of CAT, which is responsible for the formation of iodonium ions from iodide ions, thereby enabling the electrophilic reaction. When the amount of CAT was reduced or increased above the optimal value, RCP was greatly reduced (Figs. 7a and 8a). This reduction may be due to the formation of unwanted by-products at high CAT levels and insufficient oxidation of radioiodine at low CAT levels [23, 24]. RCP showed a maximum at pH 8, and RCP decreased at pH values below or above 7 (Fig. 7b and 8b), probably due to the formation of (IO-) and (IO3-) ions, which do not participate in (Formation of IO-) and (IO3-) Ion in the radioiodination process [25, 26]. At 750 µL and more of NPs values of RCP give us the highest yield, but before this value, RCP decreases (Figs. 7c and 8c) due to insufficient substrate which is required to capture all (I+) from the solution [27, 28]. Furthermore, timing is one of the key factors for optimal RCP (Figs. 7d and 8d). These data indicates that the time before 30 min is insufficient to complete the reaction. Finally, the radioiodinated nanoparticles formed were stable for more than 48 h.

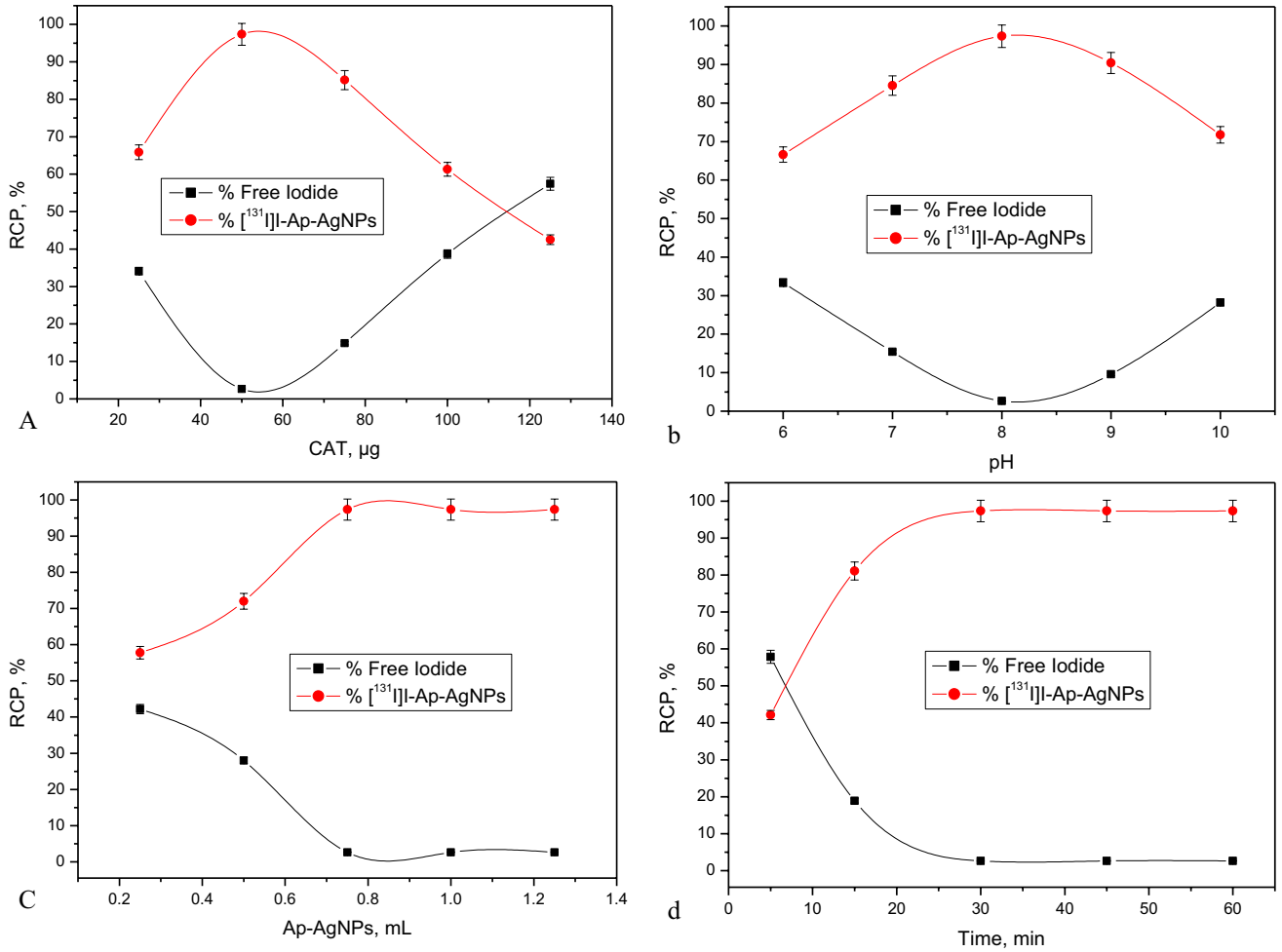

Fig. 8 Effect of reaction parameters on RCP of [^{131}I]I-Ap-AgNPs: a- CAT amount. b- pH, c- Substrate amount, d- Reaction time

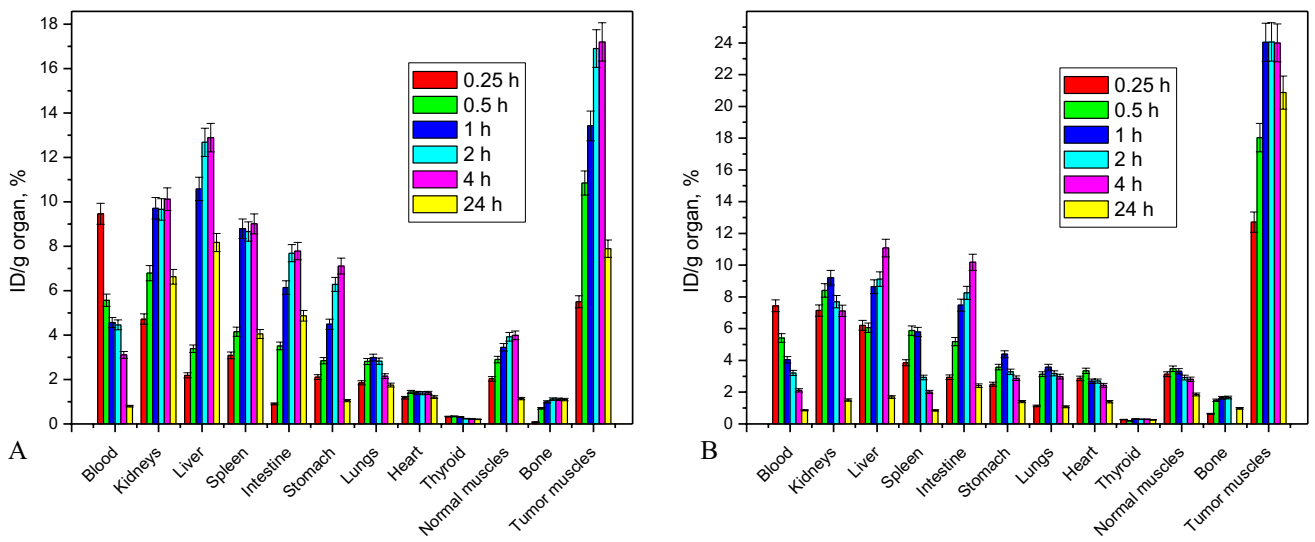

Fig. 9 Biodistribution of a- [^{131}I]I- Ch-AgNPs, b- [^{131}I]I- Ap-AgNPs in tumor bearing mice

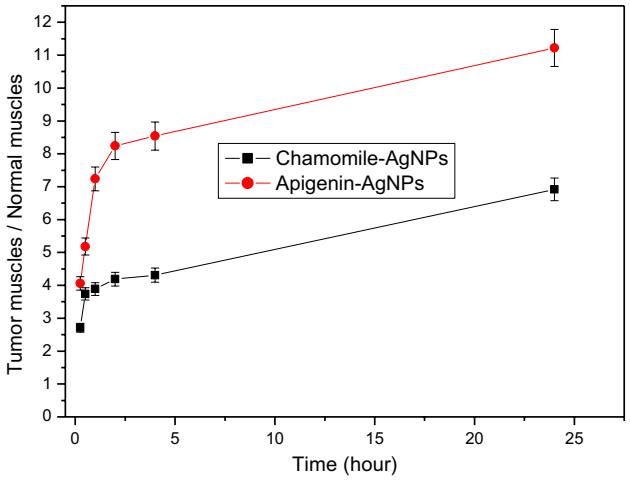

Fig. 10 Tumor muscle/Normal muscles for [^{131}I]I- Ch-AgNPs, and [^{131}I]I- Ap-AgNPs

Biodistribution study of [^{131}I]I- Ch-AgNPs and [^{131}I]I- Ap-AgNPs

Biodistribution studies of [^{131}I]I-Ch-AgNPs and [^{131}I]I-Ap-AgNPs are shown in Fig. 9a and b, respectively, at different times (0.25, 0.5, 1, 2, 4 and 24 h after injection, The elimination of both nanoplatforms was mainly through the hepatobiliary route, as the uptake in the liver was relatively high over time [29]. As shown in Fig. 9, the nanoplatforms rapidly spread to various sites due to rapid blood clearance. Regarding tumor uptake, 1 h Compared with normal muscle, [^{131}I]I-Ch-AgNPs and [^{131}I]I-Ap-AgNPs were collected at the same time in a high proportion. The tumor muscles to normal muscles ratio were shown in Fig. 10 which indicates that Ap-AgNPs accumulate in a ratio of 8.24 after two hours while the ratio in the case of Ch-AgNPs was 4.19 at the same time. These results indicates that radioiodinated NPs was able to efficiently target cancer tissue, and also indicates that both [^{131}I]I-Ch-AgNPs and [^{131}I]I-Ap-AgNPs may be used as the best opportunity for tumor theranostics.

Conclusions

Since anticancer drugs need to be developed further and more efficiently, this study aims to develop novel dual anticancer drugs that can be used in chemotherapy and radiotherapy. Ch-AgNPs and Ap-AgNPs were synthesized using a green method for in vitro chemotherapy and TRT testing. The two nanoplatforms showed high potency against the two cancer cells tested, HePG2 and HCF7, and also showed high accumulation at the cancer site, leading us to conclude that the two new formulations could be used as anticancer chemotherapeutics. These nanoplatforms can also be used for TRT by radioiodination of these platforms with ^{131}I (used as a therapeutic radioisotope). In conclusion, after further preclinical studies, the synthesized nanoplatforms can be used for chemo/radioisotope therapy.

Author contributions Conceptualization, investigation, nano-synthesis, radiolabeling, biodistribution, data curation, writing—original draft, writing—review & editing by [A.A.S.], [B.M.E.] and [I.M.A.]. Extraction, purification and analysis by I.M.A.] and [M.A.A.]. All authors read and approved the final manuscript.

Funding Open access funding provided by The Science, Technology & Innovation Funding Authority (STDF) in cooperation with The Egyptian Knowledge Bank (EKB).

Declarations

Competing interests The authors declare that they have no competing interests.

Ethical approval and consent to participate All animal procedures and experimental protocols were performed in accordance with the International Guiding Principles for Biomedical Research Involving Animals and were approved by research ethics committee, EAEA, Egypt (code: 221/27/2022). The current study adheres to the ARRIVE guidelines for reporting in vivo experiments (https://arriveguidelines.org).

References

1. Alsohaimi IH, Nassar AM, Elnasr TAS, amar Cheba B, (2020) A novel composite silver nanoparticles loaded calcium oxide stemming from egg shell recycling: a potent photocatalytic and antibacterial activities. J Clean Prod 248:119274
2. Thomas D, KurienThomas K, Latha M (2020) Preparation and evaluation of alginate nanoparticles prepared by green method for drug delivery applications. Int J Biol Macromol 154:888–895
3. Korany M, Mahmoud B, Ayoub SM, Sakr TM, Ahmed SA (2020) Synthesis and radiolabeling of vitamin C-stabilized selenium nanoparticles as a promising approach in diagnosis of solid tumors. J Radioanal Nucl Chem 325:237–244
4. Chung I-M, Rekha K, Rajakumar G, Thiruvengadam M (2018) Elicitation of silver nanoparticles enhanced the secondary metabolites and pharmacological activities in cell suspension cultures of bitter gourd. 3 Biotech 8:1–12

5. Sakr TM, Korany M, Katti KV (2018) Selenium nanomaterials in biomedicine—An overview of new opportunities in nanomedicine of selenium. J Drug Deliv Sci Technol 46:223–233
6. Molnar M, Mendešević N, Šubarić D, Banjari I, Jokić S (2017) Comparison of various techniques for the extraction of umbelliferone and herniarin in *Matricaria chamomilla* processing fractions. Chem Cent J 11:1–8
7. Srivastava JK, Gupta S (2009) Extraction, characterization, stability and biological activity of flavonoids isolated from chamomile flowers. Mol Cell Pharmacol 1:138
8. Miguel FG, Cavalheiro AH, Spinola NF, Ribeiro DL, Barcelos GRM, Antunes LMG, Hori JI, Marquele-Oliveira F, Rocha BA, Berretta AA (2015) Validation of a RP-HPLC-DAD method for chamomile (Matricaria recutita) preparations and assessment of the marker, apigenin-7-glucoside, safety and anti-inflammatory effect. Evid Based Complement Altern Med 201:89965
9. Sah A, Naseef PP, Kuruniyan MS, Jain GK, Zakir F, Aggarwal G (2022) A comprehensive study of therapeutic applications of chamomile. Pharmaceuticals 15:1284
10. Dai Y-L, Li Y, Wang Q, Niu F-J, Li K-W, Wang Y-Y, Wang J, Zhou C-Z, Gao L-N (2022) Chamomile: a review of its traditional uses, chemical constituents, pharmacological activities and quality control studies. Molecules 28:133
11. Švehlíková V, Bennett RN, Mellon FA, Needs PW, Piacente S, Kroon PA, Bao Y (2004) Isolation, identification and stability of acylated derivatives of apigenin 7-O-glucoside from chamomile (*Chamomilla recutita* [L.] Rauschert). Phytochemistry 65:2323-2332
12. Wu Q, Li W, Zhao J, Sun W, Yang Q, Chen C, Xia P, Zhu J, Zhou Y, Huang G (2021) Apigenin ameliorates doxorubicin-induced renal injury via inhibition of oxidative stress and inflammation. Biomed Pharmacother 137:111308
13. Davarpanah M, Attar Nosrati S, Khoshhosn H, Fazlali M, Kazemi Boudani M (2013) Establishment of a fast and high yield method for routine production of [131I] MIBG and investigation of its radiochemical stability for diagnosis and treatment uses. J Labell Compd Radiopharm 56:686–688
14. Jimenez C, Erwin W, Chasen B (2019) Targeted radionuclide therapy for patients with metastatic pheochromocytoma and paraganglioma: from low-specific-activity to high-specific-activity iodine-131 metaiodobenzylguanidine. Cancers 11:1018
15. Jha A, Taïeb D, Carrasquillo JA, Pryma DA, Patel M, Millo C, de Herder WW, Del Rivero J, Crona J, Shulkin BL (2021) High-specific-activity-131I-MIBG versus 177Lu-DOTATATE targeted radionuclide therapy for metastatic pheochromocytoma and paragangliomahigh-specific-activity 131I-MIBG vs. 177Lu-DOTATATE. Clin Cancer Res 27:2989–2995
16. Boly R, Lamkami T, Lompo M, Dubois J, Guissou I (2016) DPPH free radical scavenging activity of two extracts from Agelanthus dodoneifolius (Loranthaceae) leaves. Int J Toxicol Pharmacol Res 8:29–34
17. Motaleb M, Selim AA, El-Tawoosy M, Sanad M (2018) Synthesis, characterization, radiolabeling and biodistribution of a novel cyclohexane dioxime derivative as a potential candidate for tumor imaging. Int J Radiat Biol 94:590–596
18. El-Gazzar MG, Ghorab MM, Amin MA, Korany M, Khedr MA, El-Gazzar MG (2023) Computational, in vitro and radiation-based in vivo studies on acetamide quinazolinone derivatives as new proposed purine nucleoside phosphorylase inhibitors for breast cancer. Eur J Med Chem 248:115087
19. El-Masry RM, Amin MA, Korani M, Giovannuzzi S, Kadry HH, Supuran CT, Shaarawy S, Shalaby AT (2023) Elaborating 5-(4-chlorophenyl)-1, 3, 4-thiadiazole scaffold with a p-tolyl sulfonamide moiety enhances cytotoxic activity: design, synthesis, in vitro cytotoxicity evaluation, radiolabelling and in vivo pharmacokinetic study. Egypt J Chem 66:19–30
20. Johnson IT (2007) Phytochemicals and cancer. Proc Nutr Soc 66:207–215
21. Ebrahem EM, Sayed GH, Gad GN, Anwer KE, Selim AA (2022) Histopathology, pharmacokinetics and estimation of interleukin-6 levels of Moringa oleifera leaves extract-functionalized selenium nanoparticles against rats induced hepatocellular carcinoma. Cancer Nanotechnology 13:14
22. Srivastava JK, Gupta S (2007) Antiproliferative and apoptotic effects of chamomile extract in various human cancer cells. J Agric Food Chem 55:9470–9478
23. Saha GB (2012) Physics and radiobiology of nuclear medicine. Springer Science & Business Media, Singapore
24. Shewaiter MA, Selim AA, Moustafa YM, Gad S, Rashed HM (2022) Radioiodinated acemetacin loaded niosomes as a dual anticancer therapy. Int J Pharm 628:122345
25. Sakr TJR (2014) Synthesis and preliminary affinity testing of 123 I/125 I-N-(3-iodophenyl)-2-methylpyrimidine-4, 6-diamine as a novel potential lung scintigraphic agent. Radiochemistry 56:200–206
26. Essa BM, Selim AA, El-Kawy O, Abdelaziz G (2022) Preparation and preliminary evaluation study of [131I] iodocolchicine-gallic-AuNPs: a potential scintigraphic agent for inflammation detection. Int J Radiat Biol 98:1358–1365
27. Selim AA, Essa BM, Abdelmonem IM, Amin MA, Sarhan MO (2021) Extraction, purification and radioiodination of Khellin as cancer theranostic agent. Appl Radiat Isot 178:109970
28. Selim AA, Motaleb M, Fayez HA (2022) Lung cancer-targeted [131i]-iodoshikonin as theranostic agent: radiolabeling, in vivo pharmacokinetics and biodistribution. Pharm Chem J 55:1163–1168
29. Essa BM, Abd-Allah WH, Sakr TM (2022) Synthesis, 99mTc-labeling, in-vivo study and in-silico investigation of 6-amino-5-[(bis-(2-hydroxy-ethyl)-amino] methyl] 2-methyl pyrimidin-4-ol as a potential probe for tumor targeting. J Radioanal Nuclear Chem 23:1–12